Anisotropic Crystallization in Polypropylene Induced by Deformation of a Nucleating Agent Network

Aurora Nogales*,† and Geoffrey R. Mitchell

JJ Thomson Physical Laboratory, The University of Reading, Reading RG6 6AF, UK

Alun S. Vaughan

Department of Electronics and Computer Science, University of Southampton, Highfield SO17 1BJ, UK

Received March 11, 2003; Revised Manuscript Received May 12, 2003

ABSTRACT: Memory effects in propylene/ethylene copolymer (cPP) systems containing different amounts of dibenzylidene sorbitol (DBS) have been studied using wide-angle X-ray scattering techniques. It has been observed that shear flow deformation applied to the melt state containing small amounts of DBS is templated into the crystalline state. After crystallizing a sheared cPP/DBS melt, an anisotropic texture is observed by X-ray scattering, whereas the crystals produced from sheared pure cPP melts are randomly distributed. We attribute this directly to the DBS structure within the polypropylene copolymer melt. Different DBS concentrations and varying flow conditions have been explored and show that, below a certain temperature, the DBS self-organizes into a three-dimensional network within the cPP melt. When deformation is applied to this gel state, it is templated into the polymer lamellae that subsequently form, whereas when the melt is sheared at a temperature where the DBS is dissolved in the polymer, no memory of the deformation process is retained on crystallization.

Introduction

The technological processing of polymeric systems involves a variety of deformation fields, which, in general, are applied to the polymer melt. This deformation will induce a certain level of anisotropy within the polymer, and consequently, the structure that develops from such a deformed melt may differ substantially from that obtained upon crystallization from the quiescent state. Such differences may arise through several mechanisms.

First, the level of the "memory" retained in the solidified polymer from the manufacturing process will depend on the intensity and nature of the applied flow field (elongational, shear, etc.); elongational flows are considered to be more effective in terms of extending the macromolecular chains. Some of the first fundamental studies on flow-induced crystallization from solution were performed by Keller and co-workers[1,2] and revealed that shish-kebab morphologies could be induced in dilute polymer solutions using appropriate elongational flow fields. Indeed, it has generally been observed that shish-kebab-type morphologies also constitute the predominant texture[3−5] that develops when polymers are crystallized from elongated melts. In comparison with elongational flow, shear fields are considered to be much less effective at chain extension. However, even these weaker flows have the effect of perturbing chain configurations, and for high molecular weight polymers, the presence of chain entanglements does enable the shear field to produce limited chain extension.[6] Recently, several reports have presented data that demonstrate the effect of shear deformation on crystallization from sheared polymer melts.[7−11] In all these investigations, an intense shear pulse (short compared to the time taken for crystallization) was applied to samples held at the crystallization temperature, and subsequent crystallization was studied by means of time-resolved, in-situ techniques. In addition to the flow field itself, memory of deformations applied in the melt will also depend on the precise molecular characteristics of the polymer. A key factor is the relaxation behavior of the polymeric chains in the melt, and recent work has shown the importance of the molecular weight distribution in determining the morphology that evolves from a sheared melt.[9] In particular, in-situ studies have identified the role of the long molecules in defining the behavior of polydisperse systems.[11,12]

However, the molecular weight distribution may not be the only factor affecting the dynamics of a polymer melt. The presence of additives may substantially affect both its rheological properties and crystallization behavior and, hence, may exert a major influence on the material's ultimate structure and physical properties. In particular, the addition of nucleating agents to a polymeric matrix will provoke extensive changes in the crystallization process and the morphology that subsequently forms. Under quiescent conditions, the presence of small quantities of these compounds (even below 1% in weight) provides an excess of heterogeneous nuclei, which may increase the crystallization temperature of the polymer, decrease spherulitic dimensions, and change the optical and mechanical properties of the material.[13]

In the present work, the influence of a nucleating agent on the crystallization behavior of sheared polypropylene copolymer (cPP) melts is studied by means of time-resolved, in-situ, wide-angle X-ray scattering techniques. Dibenzylidene sorbitol (DBS) is a low molar mass organic compound, which promotes heterogeneous nucleation in many polyolefins at temperatures below the melting point of the polymer.[14−16] The chemical structure of DBS is shown in Figure 1. The aim of the

† Present address: Instituto de Estructura de la Materia, CSIC, Serrano 121, Madrid 28006, Spain.
* Corresponding author: E-mail emnogales@reading.ac.uk.

10.1021/ma0343028 CCC: $25.00
Published on Web 06/07/2003

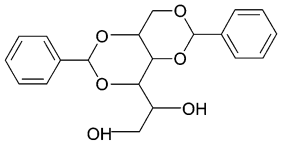

Figure 1. Chemical structure of dibenzylidene sorbitol.

present paper is therefore to establish the consequences of the presence of this particular nucleating agent for the microstructure that develops as a result of crystallizing the polymer from a deformed melt. Also, in many of the studies of shear-induced crystallization mentioned above (see, for example, refs 7−11), the shear field was applied at the crystallization temperature. Conversely, in this paper, shear deformation is applied at temperatures above the melting temperature of the polymer, and hence, crystallization from deformed melts is studied rather than shear-induced crystallization. The effect of different shear conditions on polypropylene-based samples containing DBS is discussed, and from the results obtained, a model for the behavior of the nucleating agent in this polymer melt is presented.

Experimental Section

Materials and Sample Preparation. All the systems studied in this investigation were based upon a polypropylene copolymer with $M_w = 2.2 \times 10^5$ and $M_n = 5.9 \times 10^4$ (trade name NOVOLEN 3240NC, BASF plc.), which contains 3.5% ethylene comonomer.[17] To modify its behavior, varying quantities of the nucleating agent dibenzylidene sorbitol (DBS) (trade name Millad 3905, Milliken Chemicals) were added by a solution/precipitation method, involving the initial dissolution of both components in hot xylene, followed by precipitation in an excess of isopentane/hexane. After filtration, each polypropylene/DBS system was allowed to dry at room temperature for several hours, after which time final removal of excess solvent was done by vacuum-drying at 70 °C. In this work we have used a sample code of cPP*x*, where *x* indicates the weight percentage of DBS in the system. Finally, circular disks suitable for use in the shear experiments, 1 mm in thickness and 18 mm in diameter, were prepared by melt pressing at 190 °C.

Techniques. Samples were subjected to controlled flow and thermal profiles using a parallel plate shear flow system developed at the University of Reading and described in detail elsewhere.[18] This rheometer is designed to allow scattering experiments during and following controlled shear deformations. Figure 2 shows a schematic diagram of the shear cell, together with a map of the velocity field in the sample (bottom left) and a diagrammatic representation of a typical experimental procedure (bottom right). X-ray scattering experiments were performed using two different sources, depending on the time resolution required. For steady-state measurements, a laboratory-based system was used in which the X-ray source was a sealed tube with a copper anode, operating at 1.6 kW. An incident-beam graphite crystal monochromator and pinhole collimation were employed to produce a beam ∼1 mm in diameter ($\lambda = 1.542$ Å). Time-resolved measurements were performed on beam-line 16.1 at the Synchrotron Radiation Source at Daresbury (Cheshire, UK), using a beam ∼0.4 mm in diameter ($\lambda = 1.488$ Å).

X-ray scattering data were collected using the Area X-ray Imaging System (AXIS) developed at the University of Reading,[19] in conjunction with the special rheometer outlined above. This system employs an X-ray camera with a diameter of ∼50 mm, which is based on an intensified CCD architecture complete with on-chip integration (manufactured by Photonic Science). The standard video signal from this is then passed to a frame grabber, where incoming frames are co-added to provide a more intense image with reduced statistical fluctuations. Integration times of 240 s for the laboratory source and 10 s at the synchrotron source were used. The AXIS system is highly automated, and the user can program complete sequences of events, including both flow and temperature variations, to provide X-ray scattering data directly synchronized with changes to the sample environment.[19] Azimuthual sections and radial sections were extracted from the 2-dimen-

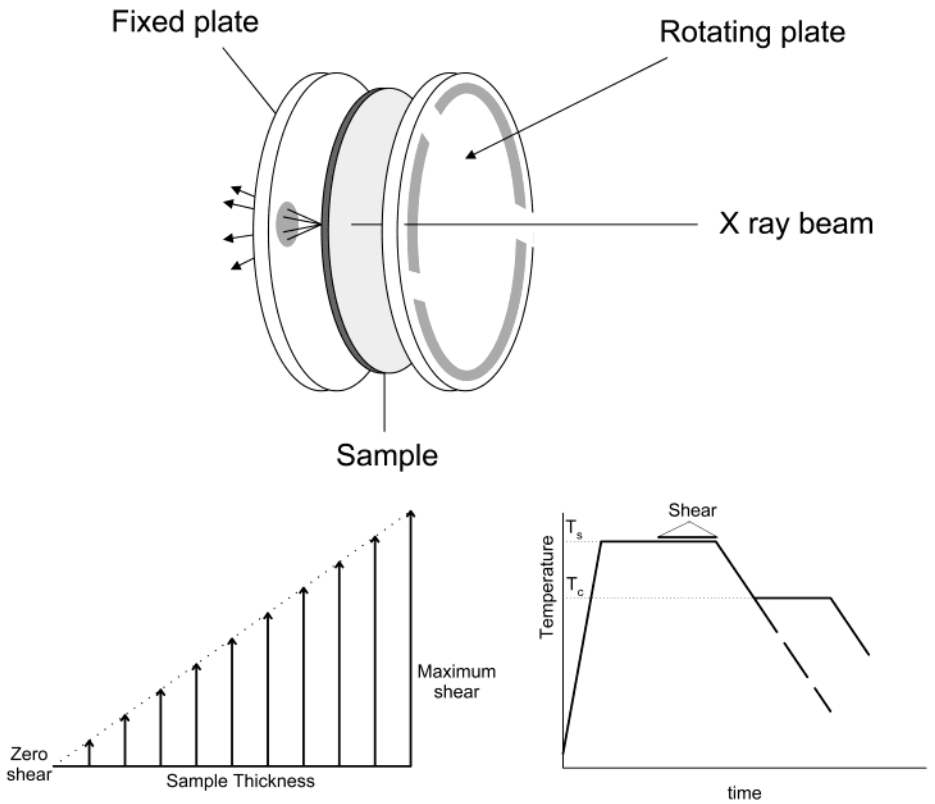

Figure 2. Schematic diagrams showing the parallel plate rheometer used for the in-situ time-resolved X-ray scattering experiments (top), the velocity map through the sample thickness (bottom right), and a typical temperature/shearing program (bottom right).

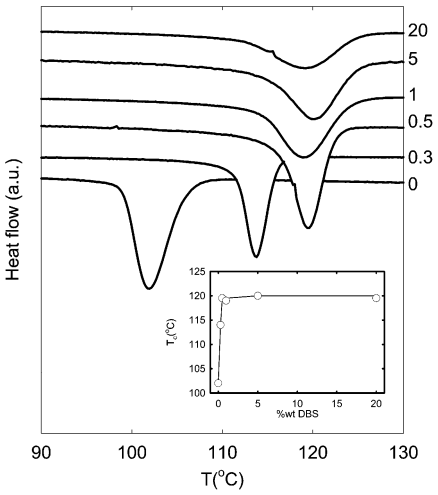

Figure 3. DSC cooling scans showing the effect of DBS content on the crystallization exotherm of the copolymer; the percentage DBS in each case is indicated by the labels. The inset shows the variation of exotherm peak maximum with DBS content.

sional scattering patterns; in all cases, the data were corrected for the detector dark count and the variable solid angle of each pixel. Azimuthual sections are plotted as a function of α, the angle between the projected scattering vector, q, and the flow axis; radial sections are plotted as a function of $|q|$, where $|q| = 4\pi \sin \theta/\lambda$, λ is the wavelength of the incident beam, and 2θ is the scattering angle.

Differential scanning calorimetry (DSC) was performed using a Perkin-Elmer DSC2 instrument at a heating rate of 10 °C/min. The temperature scale was routinely calibrated using indium and zinc standards; samples were encapsulated in aluminum pans, and the typical sample weight used in these experiments was ∼7 mg.

Results

Characterization of Samples Containing the Nucleating Agent. *Differential Scanning Calorimetry.* Figure 3 shows DSC cooling thermograms obtained from quiescent samples containing varying levels of DBS, after holding at $T_m = 190$ °C for 3 min. For the pure copolymer, cPP0, the minimum in the exothermic crystallization peak is located around $T_c = 102$ °C. However, the incorporation of only 0.3% of the nucleating agent in the polymer produces a marked shift of the crystallization peak toward higher temperatures ($T_c = 114$ °C). The inset to Figure 3 shows a plot of crystallization temperature as a function of DBS concentration, from which the largest shift in crystallization temperature from the pure polymer can be seen to occur in cPP0.5. For higher concentrations of DBS, there is a saturation in T_c, indicating that the addition of more DBS is not effective in increasing the crystallization peak temperature further, although the onset of crystallization does continue to be displaced to higher temperatures. This suggests that, at low DBS concentrations, the temperature of the crystallization peak maximum is determined, primarily, by the kinetics of nucleation, while above ∼0.5% DBS, it is the kinetics of crystal growth that dominate. Visual inspection of the samples reveals that the high DBS content systems (cPP5 and cPP20) are not optically transparent. Mitra et al.[20] studied the effect of different concentrations of DBS on the crystallization behavior and clarity of poly(ethylene terephthalate) (PET) films. As above, they observed an initial increase in crystallization temperature when

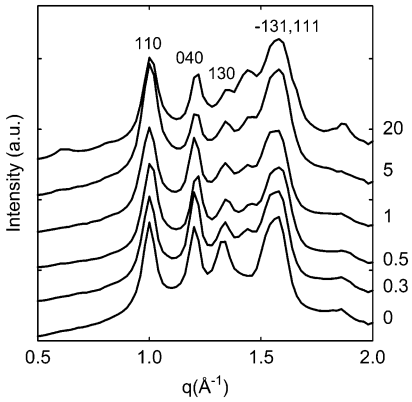

Figure 4. Plots showing wide-angle X-ray scattered intensity as a function of $|q|$ for the systems under investigation. The label to the right of each trace indicate the percentage DBS, while specific reflections, indexed according to the α−modification of polypropylene, are indicated above.

DBS is incorporated and reported that, while this increase is very strong for small concentrations of DBS, it stabilizes at higher values. The transparency of the material was also seen to decrease for DBS concentrations greater than 1%. The same authors studied the size of DBS agglomerates in amorphous polymers (polycarbonate and polystyrene) and found that their size increases linearly with the concentration of DBS.[21] The DSC results presented here may indicate that high enough amount of DBS may lead to agglomerates of DBS within the polymer matrix. From the nucleation point of view, they are not that effective in terms of free surface for the polymer chains to nucleate. Therefore, at the highest concentrations, there is a distribution of DBS fibrillar aggregates that will lead to a distribution of nucleation effectiveness. DSC heating runs show that the addition of DBS to the polypropylene matrix does not modify the melting temperature and demonstrate that all the systems under investigation here are completely molten at temperatures greater than 155 °C.

Wide-Angle X-ray Scattering. Figure 4 shows wide-angle X-ray patterns obtained from polypropylene copolymer samples containing different concentrations of DBS; all specimens were crystallized under quiescent conditions. Each of the traces shown in Figure 4 contains a series of sharp Bragg peaks, which can be indexed as follows: (110) at $|q| = 0.99$ Å^{-1}; (040) at $|q| = 1.21$ Å^{-1}; (130) at $|q| = 1.31$ Å^{-1}; overlapping (−131) and (111) peaks at $|q| \approx 1.58$ Å^{-1}. These features indicate that the crystalline structure of the sample corresponds to the α-form of isotactic polypropylene[22] and demonstrate that the polymer's unit cell is not significantly modified by the presence of the nucleating agent. In addition, there are extra peaks that accompany the inclusion of the nucleating agent. For example, in cPP5 and cPP20, small peaks are evident in the region below $|q| = 1$ Å^{-1}, while for all the samples containing DBS, regardless of concentration, a small peak appears around $|q| = 1.45$ Å^{-1}. Recent work by Foresta et al.[23] has shown that the presence of nucleating agents in similar propylene-based systems can enhance the formation of the γ−phase. Since the (117) reflection of the γ−phase of PP is located at $q = 1.42$ Å^{-1}, this extra peak may indicate the presence of the γ-phase, although from these data, this only equates to a relatively small crystalline fraction in most of the systems considered here.

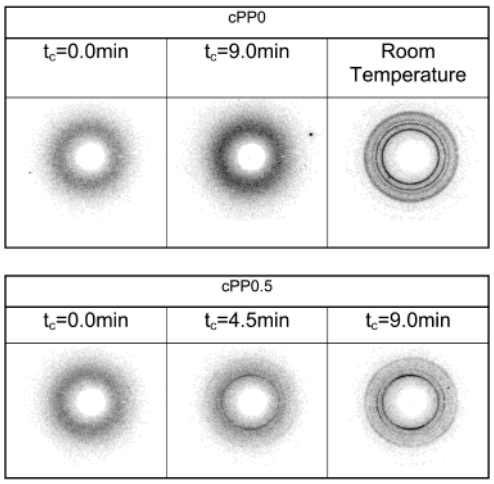

Figure 5. Wide-angle X-ray scattering patterns obtained during the crystallization of cPP0 (above) and cPP0.5 (below) at 125 °C. In the latter system, significant crystallization is evident after 4.5 min, whereas in the absence of DBS, none is detected after 9 min. The final cPP0.5 scattering pattern is also indicative of anisotropy.

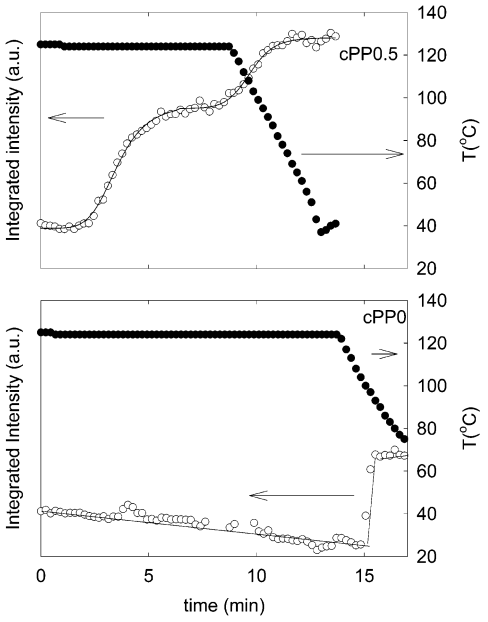

Figure 6. Plots showing the variation in integrated intensity under the (110) ring as a function of crystallization time for cPP0.5 (above) and cPP0 (below) at 125 °C. Significant isothermal crystallization can be seen in cPP0.5, whereas cPP0 only crystallizes on cooling. The same shearing conditions were imposed upon both samples.

Isothermal Crystallization of Sheared Melts Containing DBS. The isothermal crystallization of sheared polypropylene melts with and without DBS was followed in real time using wide-angle X-ray scattering techniques (WAXS). In each case, the sample was first held at $T_s = 170$ °C for 5 min to erase any memory of the preparation process from the molten polymer, after which time a defined shear flow field ($T_s = 170$ °C, $\dot{\gamma} = 1$ s^{-1}, $\gamma = 120$ su) was applied to the sample. Upon cessation of the shear flow, the sample was cooled rapidly to a selected temperature (T_c) for crystallization and held at this temperature for a given time. Throughout the shearing and postshear stages, WAXS patterns were recorded to enable the crystallization process to be monitored in a quantitative manner.

Figure 5 shows three frames taken from a sequence of WAXS patterns obtained during the isothermal crystallization of cPP0 (upper row) and cPP0.5 (lower row). Comparison of these two data sets indicates clearly that, after similarly shearing the two systems, each specimen follows a rather different crystallization path. First, there are differences in the kinetics of crystallization. After 4.5 min it is possible to detect the onset of crystallization in cPP0.5, as evidenced by the development of crystalline rings, whereas in cPP0, this is not the case even after 9 min.

This variation in overall crystallization rate is demonstrated more quantitatively in Figure 6, which compares the integrated intensity at the $|q|$ value for the (110) ring as a function of crystallization time for the cPP0 and cPP0.5 systems. In this figure, the integrated intensity also includes the scattering from the uncrystallized polymer. Consider, first, the cPP0.5 sample (Figure 6, top). After a certain induction time, the integrated (110) intensity (at $T_c = 125$ °C) exhibits a rapid increase, followed by a slowing pattern of growth, as would expected for isothermal crystallization at a relatively high temperature.[17,24,25] A further reduction in temperature produces another more rapid increase in the (110) intensity, as a result of crystallization of those ethylene-rich sequences that were rejected during the initial isothermal phase. This secondary crystallization finally levels off at ~80 °C. Consider now the behavior of cPP0, which is very different. Here, the integrated (110) intensity at $T = 125$ °C does not exhibit any increase with time, up to ~13 min, at which point the sample was cooled at ~16 °C/min down to room temperature. During cooling, crystalline reflections are first observed at ~100 °C, after which a sudden jump in the (110) intensity is seen. When the different cooling rates are taken into account, these X-ray results are in broad agreement with the DSC cooling scans shown in Figure 3.

However, the X-ray scattering data presented in Figure 5 show, in addition to the change in crystallization kinetics, that the addition of DBS also results in the formation of an anisotropic crystal texture. The initial X-ray scattering patterns obtained from the two samples are composed of diffuse rings, corresponding to the amorphous halo of the molten polymer, but as crystallization proceeds, discrete reflections appear which correspond to the Bragg reflections of the α-form of polypropylene. In the case of the cPP0.5 specimen, the azimuthal distribution of intensity around these Bragg rings is clearly nonuniform. Conversely, the cPP0 sample exhibits an isotropic azimuthal distribution of intensity throughout the crystallization, indicating that, in this system, the crystals are randomly oriented. Evidently, the cPP0.5 sample displays some memory effect relating to the deformation applied in the melt, whereas the cPP0 specimen does not.

Relationships between DBS Content and Anisotropy. A systematic series of samples of cPP/DBS with differing DBS content were subjected to the same shearing conditions (i.e., $T_s = 160$ °C, $\dot{\gamma} = 20$ s^{-1}, $\gamma = 120$ su) and then cooled rapidly to room temperature. The WAXS patterns subsequently obtained at room temperature are presented in Figure 7. Other than for cPP0, each of these patterns shows a distinct level of anisotropy, even for samples containing only a small fraction of DBS. Examination of the azimuthal variation in intensity for the various crystalline reflections reveals that the pattern of anisotropy or texture is the same in

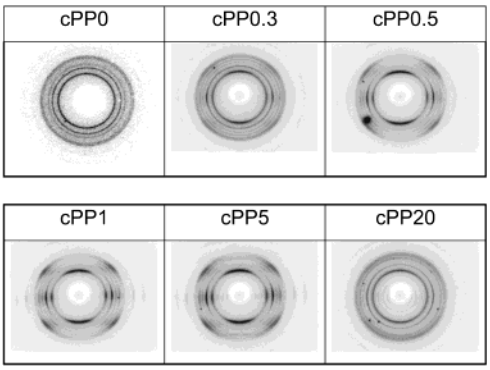

Figure 7. Room temperature wide-angle X-ray scattering patterns obtained from samples containing different amounts of DBS. From these, the extent of anisotropy increases with DBS content, with the notable exception of cPP20 (20% DBS). All samples were sheared at $T_s = 160$ °C, $\dot{\gamma} = 20$ s^{-1}, and $\gamma = 120$ su and then cooled rapidly to room temperature.

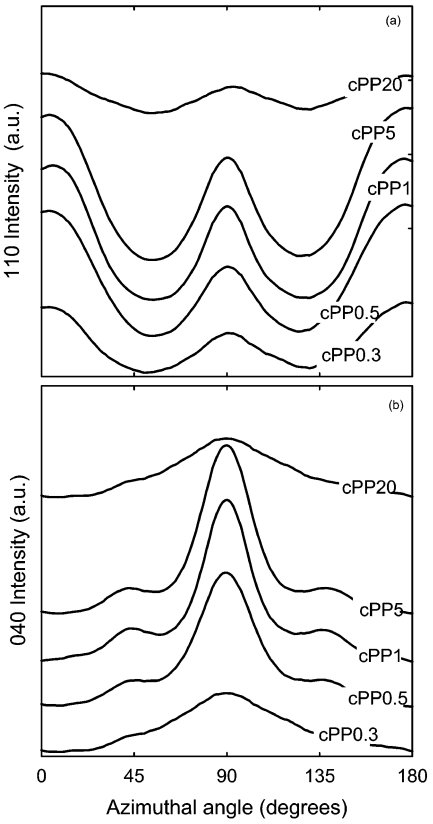

Figure 8. Traces showing the variation in intensity of the (110) and (040) reflections as a function of the azimuthal angle, for cPP*x* samples containing different concentrations of DBS. The extent of anisotropy increases with DBS content, with the notable exception of cPP20 (20% DBS). All samples were sheared in the melt at $T_s = 160$ °C, $\dot{\gamma} = 20$ s^{-1}, and $\gamma = 120$ su.

all cases, although the levels of anisotropy that are observed do depend on DBS concentration. In Figure 8, the intensity of the (110) and (040) reflections are presented as a function of azimuthal angle for the different samples, after being cooled rapidly to room temperature. The data for cPP0 are not shown, since it is invariant with azimuthal angle. For each of the other samples, regardless of the DBS concentration, the (110) intensity curve shows maxima in the meridian (azimuthal angle, $\alpha = 0°$) and in the equator ($\alpha = 90°$). In contrast, the (040) intensity curves exhibit a maximum in the equator ($\alpha = 90°$) and a minimum in the meridian

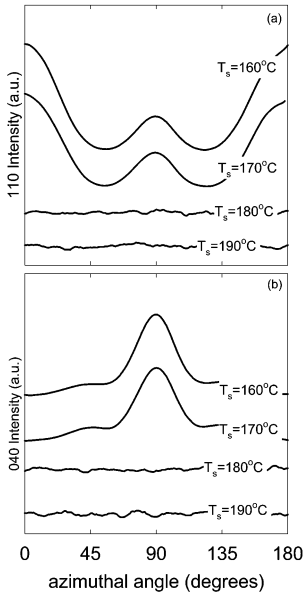

Figure 9. Traces showing the variation in intensity of the (110) and (040) reflections as a function of shearing temperature, T_s, for cPP0.5; above $T_s = 170$ °C, the scattering patterns are isotropic. In all cases, the material was sheared using $\dot{\gamma} = 20$ s^{-1} and $\gamma = 120$ su.

($\alpha = 0°$). The strength of the azimuthal variations reflects the level of preferred orientation of the polypropylene crystals, and with the notable exception of the specimen containing the greatest amount of DBS (sample iPP20), the level of preferred orientation increases with the concentration of the nucleating agent.

Influence of Shearing Conditions on Anisotropy. *Melt Temperature.* A series of cPP0.5 samples were sheared at different temperatures above the polymer's melting point, using the same shear conditions as above ($\dot{\gamma} = 20$ s^{-1}, $\gamma = 120$ su), and then cooled rapidly to room temperature. The azimuthal variation of the (110) and (040) reflections taken at room temperature for this series of samples is shown in Figure 9. Samples sheared at a high temperature show an isotropic distribution of intensity despite the prior imposition of a flow field. However, when the shearing is performed at $T_s = 170$ °C or below, a highly anisotropic X-ray pattern is obtained, demonstrating that such samples develop an oriented texture on crystallizing. One possibility to account for this transition around $T = 170-180$ °C is that it is related to the state of the DBS in the polymer melt at the time of shearing.

Shear Rate. As with all deformations, shear flow involves both the rate (shear rate) and the extent of deformation (shear strain). To help differentiate between these two factors, different shear rates ($\dot{\gamma} = 0.5$, 1, and 20 s^{-1}), but the same shear strain ($\gamma = 20$ su), were applied to a series of cPP0.5 samples held at $T_s = 160$ °C. After finishing the shear program, the specimens were cooled rapidly to room temperature and examined by WAXS. All samples exhibit an anisotropic crystalline texture at room temperature, regardless of the applied shear rate; the azimuthal intensity distribution of the (110) and (040) reflections are shown in Figure 10. From this, it is clear that the amount of oriented crystals is greater in samples subjected to higher shear rates ($\dot{\gamma} = 1$ and 20 s^{-1}), although some of anisotropy is still observed in the sample that had been sheared at $\dot{\gamma} = 0.5$ s^{-1}.

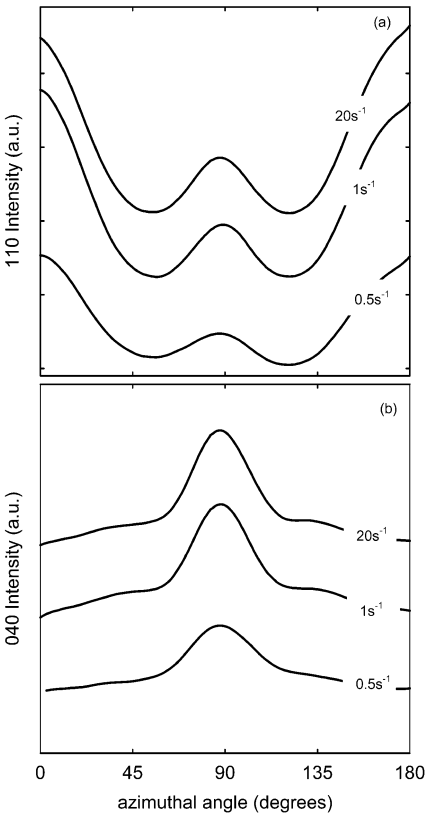

Figure 10. Traces showing the variation in intensity of the (110) and (040) reflections as a function of shear rate for cPP0.5; shear conditions of $\gamma = 120$ su and $T_s = 160$ °C were used in all cases. From these plots, it is evident that anisotropy increases with shear rate.

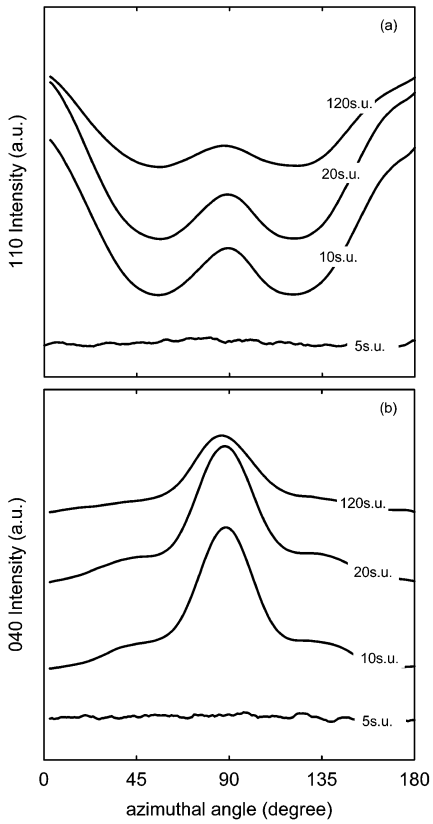

Figure 11. Traces showing the variation in intensity of the (110) and (040) reflections as a function of shear strain for cPP0.5; shear conditions of $\dot{\gamma} = 1$ s^{-1} and $T_s = 160$ °C were used in all cases. From these data, it is evident that increasing the shear strain initially results in an increase in anisotropy. However, for $\gamma = 20$ su, the anisotropy in the WAXS pattern is significantly reduced.

Shear Strain. A series of samples of cPP0.5 were prepared at $T_s = 160$ °C using different shear strains ($\gamma = 5$, 10, 20, and 120 su) but a constant shear rate of $\dot{\gamma} = 1$ s^{-1}. After the cessation of shear flow, the samples were again cooled rapidly to room temperature for study. Figure 11 shows the azimuthal intensity variations for the (110) and (040) reflections as a function of shear strain. At very low shear strains, $\gamma = 5$ s^{-1} in Figure 11, the WAXS intensity is isotropic. However, as the shear strain increases, the WAXS patterns exhibit more anisotropic distributions of intensity although, for the highest shear strain sample ($\gamma = 120$ su), the anisotropy in the WAXS pattern is significantly reduced.

Dependence of Preferred Orientation on Shearing Conditions and Sample Composition. In polymers related to polypropylene, quantification of the amount of oriented material is complicated by the nature of the lamellar texture that forms in these systems. Consequently, to provide an estimate of the anisotropy generated by the different shearing conditions in the different samples, we have chosen to calculate the area under each (110) azimuthal curve, after subtracting the isotropic scattering. While the values obtained are not an absolute measure of orientation, they do allow trends in behavior to be identified. A summary of the dependence of this measure of orientation upon shearing conditions and sample composition is presented in Figure 12.

Discussion

The in-situ X-ray experiments reported above set out to characterize the structural and morphological differences that result from crystallizing a polypropylene-based copolymer from a presheared melt, with and without DBS as a nucleating agent. Comparing the isothermal crystallization behavior of a DBS-modified cPP melt (cPP0.5) with that of nonmodified cPP (cPP0) reveals that the presence of DBS in the melt produced two main effects. The first relates to the nucleating effectiveness of the DBS. The DBS accelerates crystallization by reducing the induction time. This finding is in agreement with previous studies, for example ref 17, where it was shown that the DBS massively increases the number of nucleation sites. In cPP, these sites prevent the appearance of a spherulitic texture and produce a uniform lamellar morphology when crystallization occurs below a critical temperature ($T_c < 128$ °C for the present copolymer system). The second effect is new and very striking. We have shown that the cPP melt only retains a memory of the applied shear deformation, which manifests itself through the formation of anisotropic morphologies, when DBS is present (see Figure 5). As shown in Figure 5, the cPP without DBS does not develop an anisotropic distribution of crystal orientation when crystallized from a sheared melt. For the DBS containing sample, the shear flow develops some level of anisotropy in the melt, and this anisotropy acts as a template for the process of polymer crystallization, producing obvious levels of anisotropy. Previous work on DBS-free polyethylene[26,27] revealed that shearing the melt leads to extremely small levels of global orientation, but by crystallizing from this sheared melt, the level of anisotropy of the crystalline

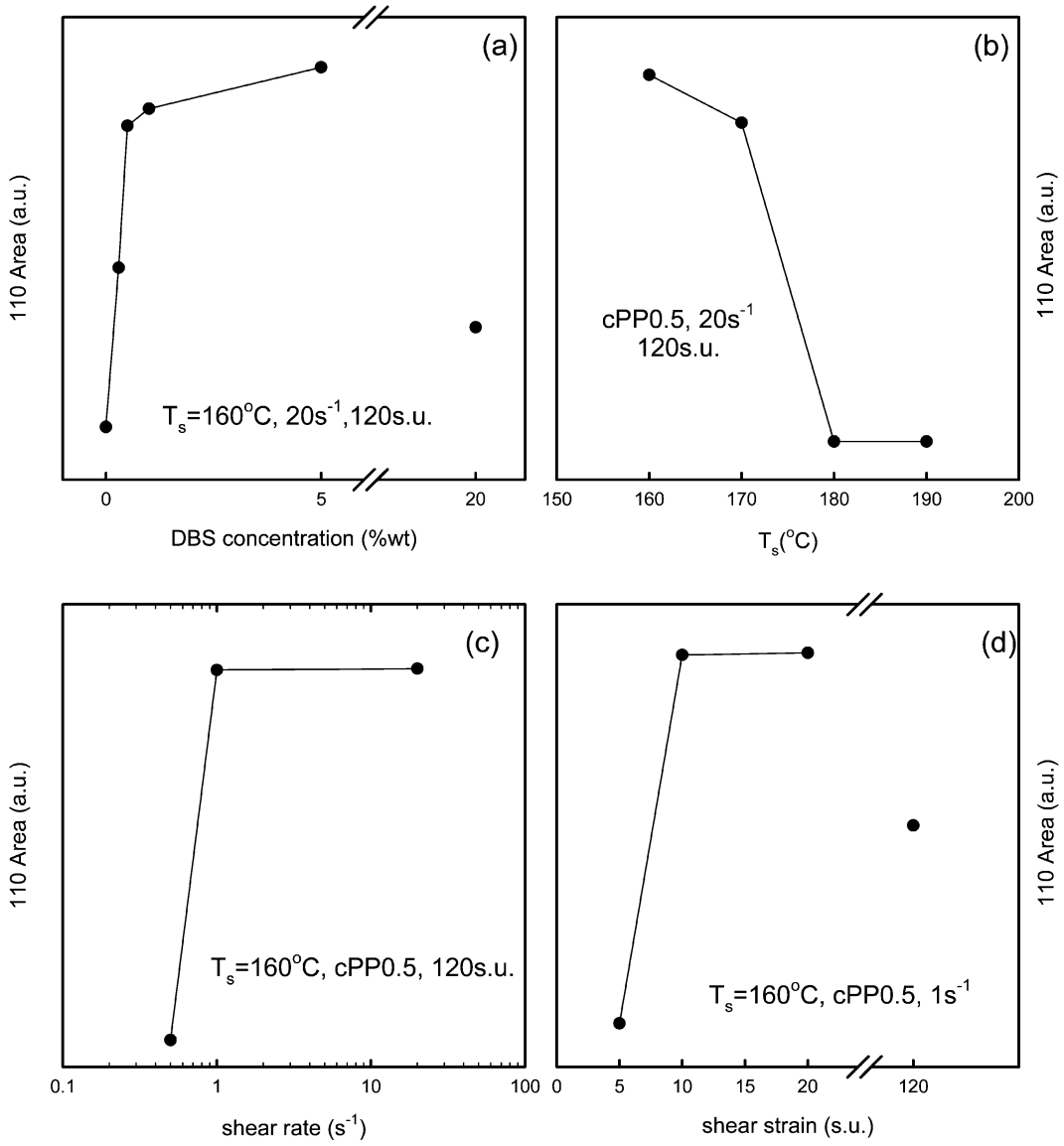

Figure 12. Dependence of the orientation, evaluated in terms of the area under the azimuthal (110) curve, on (a) DBS concentration, (b) shear temperature, (c) shear rate, and (d) shear strain.

texture is increased by an order of magnitude. In that work,[26,27] the extent of templating the "memory" of shear deformation in the melt onto the crystallized sample was shown to depend on the molecular characteristics of the polymer, specifically the molecular weight distribution. However, in the particular case treated here, the "memory" effect is dependent upon the presence of the nucleating agent. Two possibilities might be considered. On one hand, one may speculate that the orientation memory imposed by the presence of the nucleating agent is due to a shift in the temperature range for the maximum crystallization rate of polypropylene. It has been suggested that, in its early stages, crystallization can be viewed as a physical gelation process.[28,29] As the crystallization temperature is varied, the time to reach the gel point decreases exponentially with the undercooling ($T_m - T_c$).[29] The addition of the nucleating agent would produce an enhancement of this behavior. Therefore, in the cPP/DBS system, at lower temperatures, the melt may contain some nuclei or other objects that act as physical cross-links. These would not be found in the equivalent pure cPP system. However, if this were the appropriate model, similar memory effects would also be observed when shearing cPP melts with other nucleating agents. We have made tests with other nucleating agents, most notably a similar propylene−ethylene copolymer nucleated by Borealis using their proprietary technique,[30] and have observed no memory type effects. Also, some preliminary results obtained in DBS modified polyethylene has led to a similar conclusion. Shearing those systems at temperatures about the theoretical melting point of polyethylene but below the estimated temperature of formation of the DBS network (170 °C) produces orientation of the semicrystalline polymer upon cooling.[31]

Recent studies have shown that DBS induces thermoreversible gelation in several common low molar mass solvents.[32−36] It is thought that DBS self-assembles through hydrogen bonding, even at relatively low concentrations, forming a three-dimensional percolation network in low molecular weight solvents. The critical gel concentration and the morphology of the DBS network have been found to be highly dependent on the polarity of the solvent.[32] DBS also produces physical gelation when small concentrations are added to polymeric solvents, such as poly(dimethylsiloxane), poly(propylene glycol), and poly(propylene oxide).[37,38] Shepard et al. have reported the evolution of the complex

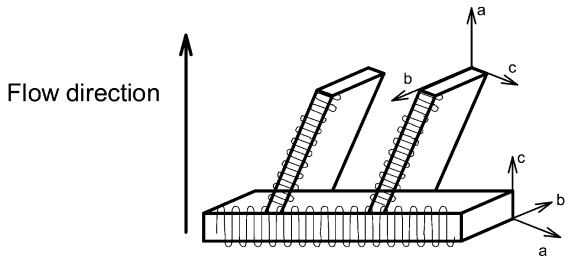

Figure 13. Schematic diagram to indicate the relationships between the observed WAXS scattering patterns and the polymer's underlying lamellar texture. DBS fibrils are oriented along the flow direction; the parent lamella nucleates through an epitaxial interaction with the DBS fibrils and is oriented perpendicular to the flow direction; daughter lamellae are oriented in a direction that is close to parallel to the flow but is defined by the parent lamella.

viscosity as a function of temperature for an equivalent propylene/ethylene copolymer to that studied here, modified with different concentrations of 1,3:2,4-di-*p*-methylbenzylidene sorbitol (MDBS).[39] They observe a pronounced increase in the intrinsic viscosity upon cooling the polymer melt prior to crystallization. The authors attributed this increase to the formation of a network of MDBS nanofibrils; the temperature at which this increase in viscosity occurred was found to be MDBS concentration dependent. The above results, therefore, support the hypothesis of DBS-modified polymer systems undergoing a sol−gel transition at a certain temperature, which will depend on sample history and composition. Below this temperature (in this work, 170 °C < T_s < 180 °C), DBS self-assembles into some structures (probably a fibrillar network) that become oriented by the shear process. This oriented structure, even at very low concentrations, templates or directs the cPP crystallization process, as indicated by the azimuthal orientation distribution of the crystalline polypropylene reflections.

For all nonzero concentrations of DBS, crystallization from a presheared DBS-modified polymer melt leads to significant anisotropy in the resultant room temperature sample (Figure 7). In all cases, this relates to the same underlying lamellar texture. In such samples, the innermost cPP reflection, (110), is more intense near the meridian, but with some intensity in the equator. Conversely, the (040) reflection is most intense in the equator and, for the highly aligned samples, presents virtually zero intensity in the meridian. This type of WAXS texture arises from a crosshatched structure[40] of parent and daughter lamellae, where the secondary or daughter lamellae nucleate and grow from previously formed primary lamellae (the parents). An idealized model of this arrangement is presented in Figure 13. This model would account for the observed (040) intensity on the equator, since the *b*-axes of both parent and daughter lamellae are perpendicular to the flow direction. Also, from this, the (110) intensity corresponding to the parent lamellae would be concentrated in the equator, since the *c*-axes of the parent lamellae are parallel to the flow direction, while the (110) intensity for the daughter lamellae would lie close to the meridian; the *c*-axes of the daughter lamellae are nearly perpendicular to the flow direction.

This model appears to be reasonable in relation to the orientation of the polymer lamellae that develop in the DBS-modified copolymer. Assuming that the DBS does indeed form fibrils, these will have a high surface area[41] and, during the shear process, will tend to be aligned in the direction of the shear flow. Indeed, we have some evidence for the alignment of DBS crystals during shear flow from the observed WAXS patterns. These fibrils will then assist polymer chains, upon cooling, to nucleate and form the primary lamellae, through some form of epitaxy, with the consequence that the cPP chains that form the parent lamellae will lie parallel to the axis of the filaments. Thierry et al.[42] have reported that polyethylene vapor deposited on DBS filaments displays fiber diffraction patterns, from which they similarly imply an epitaxial interaction between the polymer and the DBS. Our model for the results we have observed is therefore based upon the notion that it is only a very small fraction of the material under investigation that responds to the flow field but that this subsequently acts to template anisotropy onto the whole polymer system. In this case, the small but critical fraction of the system corresponds to the high surface area assemblies of DBS.

Using the above model, it is now possible to explain the different levels of anisotropy obtained under different shearing conditions. Clearly, without any DBS there is no anisotropy. Similarly, shearing the DBS modified cPP melts at temperatures above the sol−gel transition (Figure 12b) does not lead to anisotropy; no fibrils of DBS are present. At the transition temperature (between 170 and 180 °C), the DBS self-assembles and forms a percolating fibrillar network that absorbs the deformation and templates, upon cooling, the subsequent polymer crystals. At a given temperature below the transition temperature, deforming the melt at different shear rates induces anisotropy. However, for very low shear rates the orientation is very low, suggesting that some sort of relaxation of the alignment of the DBS fibrils occurs. However, for shear rates above a threshold, the orientation is almost independent of the shear rate (Figure 12c). The orientation exhibits a more complicated dependence upon shear strain. Very small shear strains do not produce anisotropy. Intermediate shear strains produce high levels of anisotropy. However, for very high shear strains the orientation is reduced, suggesting a breakage of the fibril network due to an excess of strain (Figure 12d). The orientation also presents some dependence upon the DBS concentration (Figure 12a). For DBS concentrations up to 5%, under the same shearing conditions, the orientation increases with DBS concentration. However, the sample cPP20 exhibits a very low orientation when deformed under the same shearing conditions. This effect can be explained by taking into account DBS structures other than fibrils, which may form at such high concentrations.

Conclusions

Modest shear flow deformation applied to cPP samples modified by the addition of very small quantities of dibenzylidene sorbitol leads to highly anisotropic textures in the final semicrystalline sample at room temperature. The results presented here support the view that DBS forms a three-dimensional network at temperatures below a given transition temperature. Below this transition temperature, the DBS modified polymer melts can be envisioned as a gel system. When this gel system is sheared, the orientation induced in the melt is templated and multiplied at lower temperature when the polymer crystallized. The proposed model consists of a system of DBS fibrils, which become aligned in the

flow direction. These aligned fibrils, due to their high surface area, nucleate primary cPP lamellae upon cooling by means of epitaxial interactions, where the cPP chains are positioned parallel to the fibril axis. There is also a population of daughter lamellae that grow onto the surface of the parent one.

Acknowledgment. A.N. thanks the support of this research by a Marie Curie Fellowship of the European Union programme "Human Potential" under Contract HPMF-CT-2000-00657. The synchrotron-based X-ray experiments were performed at the CCLRC Daresbury SRS facility.

References and Notes

(1) Pope, D. P.; Keller, A. *Colloid Polym. Sci.* **1978**, *256*, 751.
(2) Miles, M. J.; Keller, A. *Polymer* **1980**, *21*, 1295.
(3) Keller, A.; Kolnaar, H. W. H. *Mater. Sci. Technol.* **1997**, *18*, 189.
(4) Eder, G.; Janeschitz-Kriegl, H.; Liedauer, S. *Prog. Polym. Sci.* **1990**, *15*, 629.
(5) Jerschow, P.; Janeschitz-Kriegl, H. *Int. Polym. Process.* **1997**, *12*, 72.
(6) Keller, A.; Kolnaar, H. W. H. In *Processing of Polymers*; Meijer, H. E. H., Ed.; VCH-Wiley: Weinheim, 1997; Vol. 18, Chapter 4, pp 189−268.
(7) Kumaraswamy, G.; Issaian, A. M.; Kornfield, J. A. *Macromolecules* **1999**, *32*, 7537.
(8) Kumaraswamy, G.; Verma, R. K.; Issaian, A. M.; Wang, P.; Kornfield, J. A.; Yeh, F.; Hsiao, B. S.; Olley, R. H. *Polymer* **2000**, *41*, 8931.
(9) Somani, R.; Nogales, A.; Hsiao, B. S.; Srinivas, S.; Tsou, A. H.; Sics, I.; Ezquerra, T. A.; Balta Calleja, F. J. *Macromolecules* **2000**, *33*, 9385.
(10) Somani, R. H.; Hsiao, B. S.; Nogales, A.; Fruitwala, H.; Srinivas, S.; Tsou, A. H. *Macromolecules* **2001**, *34*, 5902.
(11) Nogales, A.; Hsiao, B. S.; Somani, R.; Srinivas, S.; Tsou, A. H.; Balta Calleja, F. J.; Ezquerra, T. A. *Polymer* **2001**, *42*, 5247.
(12) Seki, M.; Thurman, D. W.; Oberhauser, J. P.; Kornfield, J. A. *Macromolecules* **2002**, *35*, 2583.
(13) Jansen, J. In *Plastic Additive Handbook*; Gächter and Müller, Eds.; Chapter 18.
(14) Kim, Y. C.; Kim, C. Y.; Kim, S. C. *Polym. Eng. Sci.* **1991**, *31*, 1009.
(15) Kim, C. Y.; Kim, Y. C.; Kim, S. C. *Polym. Eng. Sci.* **1993**, *33*, 1445.
(16) Fujiyama, M.; Wakino, T. *J. Appl. Polym. Sci.* **1991**, *42*, 2739.
(17) Zhao, Y.; Vaughan, A. S.; Sutton, S. J.; Swingler, S. G. *Polymer* **2001**, *42*, 6587.
(18) Nogales, A.; Thornley, S. A.; Mitchell, G. R. *J. Macromol. Sci., Phys.*, in press.
(19) Pople, J. A.; Mitchell, G. R.; Chai, C. K. *Adv. X-Ray Anal.* **1995**, *38*, 531.
(20) Mitra, D.; Misra, A. *J. Appl. Polym. Sci.* **1988**, *36*, 387.
(21) Misra, A.; Mitra, D. *Polymer* **1988**, *29*, 1990.
(22) Varga, J. In *Polypropylene: Structure, Blends and Composites*; Karger Kocsis, J., Ed.; Chapman & Hall: London, 1995; p 56.
(23) Foresta, T.; Piccarolo, S.; Goldbeck-Wood, G. *Polymer* **2001**, *42*, 1167.
(24) Schultz, J. M. *Polymer Materials Science*; Prentice Hall: New York, 1974.
(25) Zachmann, H. G.; Wutz, C. *Crystallisation of Polymers*; Dosiere, M., Ed.; Kluwer Academic Publishers: Dordrecht.
(26) Pople, J. A.; Mitchell, G. R.; Chai, C. *Polymer* **1996**, *37*, 4187.
(27) Pople, J. A.; Mitchell, G. R.; Sutton, S. J.; Vaughan, A. S.; Chai, C. *Polymer* **1999**, *40*, 2769.
(28) Schwittay, C.; Mours, M.; Winter, H. H. *Faraday Discuss.* **1995**, *101*, 93.
(29) Pogodina, N. V.; Winter, H. H. *Macromolecules* **1998**, *31*, 8164.
(30) Nogales, A.; Mitchell, G. R., unpublished results.
(31) Nogales, A.; Mitchell, G. R. Poster presented in the European Physical Society Conference: Polymers and Synchrotron Radiation, Sheffield, 2002.
(32) Yamasaki, S.; Tsutsumi, H. *Bull. Chem. Soc. Jpn.* **1995**, *68*, 123.
(33) Yamasaki, S.; Ohashi, Y.; Tsutsumi, H.; Tsujii, K. *Bull. Chem. Soc. Jpn.* **1995**, *68*, 146.
(34) Yamasaki, S.; Tsutsumi, H. *Bull. Chem. Soc. Jpn.* **1994**, *67*, 906.
(35) Yamasaki, S.; Tsutsumi, H. *Bull. Chem. Soc. Jpn.* **1994**, *67*, 2053.
(36) Yamasaki, S.; Tsutsumi, H. *Bull. Chem. Soc. Jpn.* **1996**, *69*, 561.
(37) Mercurio, D. J.; Spontak, R. J. *J. Phys. Chem. B* **2001**, *105*, 2091.
(38) Nunez, C. M.; Whitfield, J. K.; Mercurio, D. J.; Ilzhoefer, J. R.; Spontak, R. J. *Macromol. Symp.* **1996**, *100*, 275.
(39) Shepard, T. A.; Delsorbo, C. R.; Louth, R. M.; Walborn, J. L.; Norman, D. A.; Harvey, N. G.; Spontak, R. J. *J. Polym. Sci., Part B: Polym. Phys.* **1997**, *35*, 2617.
(40) Lotz, B.; Wittmann, C. *J. Polym. Sci., Part B: Polym. Phys.* **1986**, *24*, 1541.
(41) Thierry, A.; Fillon, B.; Straupe, C.; Lotz, B.; Wittmann, J. C. *Prog. Colloid Polym. Sci.* **1992**, *87*, 28.
(42) Thierry, A.; Straupe, C.; Lotz, B.; Wittmann, J. C. *Polym. Commun.* **1990**, *31*, 299.

MA0343028